

# Targeting Abasic Sites in DNA by Aminoalkyl-Substituted Carboxamidoacridizinium Derivatives and Acridizinium–Adenine Conjugates

Katja Benner,<sup>[a]</sup> Anton Granzhan,<sup>[a]</sup> Heiko Ihmels,<sup>\*,[a]</sup> and Giampietro Viola<sup>[b]</sup>

*Dedicated to Professor Adalbert Maercker on the occasion of his 75th birthday*

**Keywords:** Nitrogen heterocycles / Acridizinium / Adenine / DNA recognition / Abasic DNA

Two isomeric acridizinium–adenine conjugates, along with three model compounds (i.e. two 9-(*N*-alkylcarboxamido)-acridizinium salts and one 9-{*N*-[(dimethylamino)alkyl]-carboxamido}acridizinium salt) were prepared from the corresponding carboxyacridizinium salts. The interaction of these compounds with calf thymus DNA was studied by spectrophotometric and viscosimetric titrations, LD spectroscopy, and thermal DNA denaturation experiments. Both of the acridizinium–adenine conjugates and the *N*-alkyl-carboxamides intercalate into calf thymus DNA with moderate affinity [ $K \approx 10^4 \text{ M}^{-1}$  (DNA concentration in bp)]. In contrast, the *N*-[3-(dimethylamino)propyl]-substituted carboxamide exhibits a significantly higher binding constant under identical conditions ( $K \approx 10^5 \text{ M}^{-1}$ ). The association of the acridizinium derivatives with abasic-site containing DNA was assessed by thermal denaturation experiments with synthetic

double-stranded oligonucleotides, which contained one (TX) or no abasic site (TA). The acridizinium–adenine conjugates stabilize the DNA with the abasic position slightly more than they do the regular duplex, as indicated by the difference of the induced melting-temperature shifts between the TX and TA duplexes ( $\Delta\Delta T_m \approx 4^\circ\text{C}$ ) at a ligand/DNA ratio  $r$  of 0.5. Most notably, a significantly more efficient stabilization ( $\Delta\Delta T_m = 9.6^\circ\text{C}$ ) of the abasic duplex is achieved by the aminoalkyl derivative, namely 9-{*N*-[3-(dimethylamino)-propyl]carboxamido}acridizinium salt, which does not carry an adenine substituent. These results indicate that the design of abasic-site-targeting ligands must not necessarily involve the attachment of a nucleic acid base to the DNA intercalator.

(© Wiley-VCH Verlag GmbH & Co. KGaA, 69451 Weinheim, Germany, 2007)

## Introduction

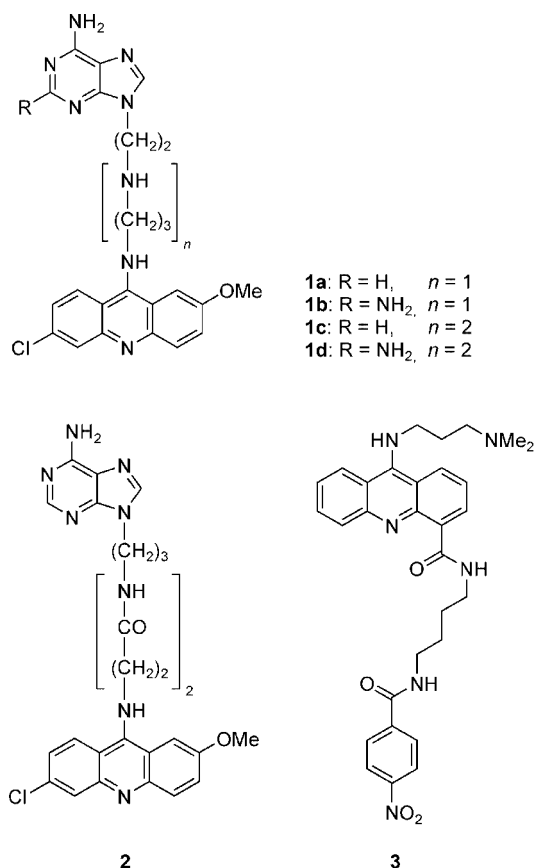
Abasic sites, apurinic or apyrimidinic (AP) sites, are commonly observed mutagenic or carcinogenic DNA lesions.<sup>[1]</sup> They are formed as intermediates either in the enzymatic repair of damaged DNA (e.g. during the removal of modified nucleic acid bases), or by the influence of exogenous factors.<sup>[2]</sup> Recently, attempts have been made to design molecules which bind to AP sites selectively and interfere with the enzymatic repair processes of the AP endonucleases. Although this process is not desired in healthy tissue, the suppression of DNA repair may be employed to assist antitumor drugs, whose efficiency is reduced by the cellular repair of the drug-induced DNA damage.<sup>[3]</sup> Among the most promising lead structures,<sup>[4]</sup> that were designed to bind selectively to abasic sites, are the intercalator–nucleic acid base conjugates such as **1** and **2**.<sup>[1,5]</sup> These compounds include (i) a nucleic acid base that intercalates into the

abasic site and forms hydrogen bonds with the nucleic acid base in the opposite strand; (ii) a DNA intercalator, which provides a significant, but non-specific affinity for DNA; and (iii) a linker unit with DNA-binding and/or DNA-cleaving properties. These molecules may act as artificial nucleases or inhibitors of DNA repair.<sup>[6]</sup> Notably, recent studies have shown that the nucleic base is not absolutely necessary for the action of the AP site binders of the described type. Thus, compound **3**, in which the nucleic acid base is omitted, also binds preferentially to abasic DNA sites and induces DNA photocleavage in their proximity.<sup>[7]</sup>

In our efforts towards the establishment of annealed quinolizinium derivatives (acridizinium) as a versatile platform for DNA-targeting drugs,<sup>[8]</sup> we intended to synthesize acridizinium–nucleobase conjugates. We proposed that such conjugates may, as do compounds **1** and **2**, represent a class of abasic site binders. However, in contrast to **1** and **2** the acridizinium–nucleobase conjugates may also be used to induce DNA lesions close to the abasic site upon irradiation with near-UV light, since it has been shown that the acridizinium ion acts as an efficient photosensitizer.<sup>[9]</sup> Herein we present the synthesis of acridizinium–adenine conjugates and acridizinium carboxamides, along with the first studies

[a] Universität Siegen, Organische Chemie II, Adolf-Reichwein-Str. 2, 57068 Siegen, Germany  
Fax: +49-271-740-4052  
E-mail: ihmels@chemie.uni-siegen.de

[b] Department of Pharmaceutical Sciences, University of Padova, Via Marzolo 5, 35131, Italy

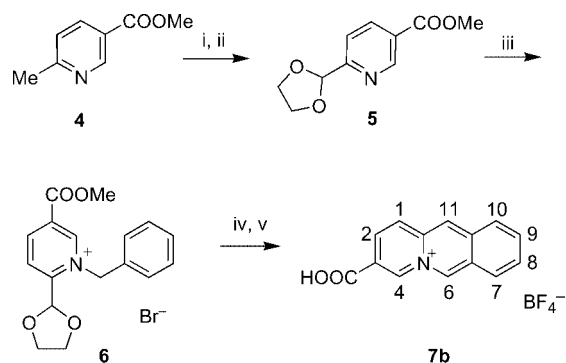


on the DNA-binding properties of these compounds. Although it is well known that the binding affinity of conjugates to abasic sites is enhanced by the amino groups of the linker due to the increased positive charge of the ligand upon protonation, we chose to employ amide functionalities instead for the construction of the linker. Since the amino functionality may induce DNA-strand cleavage close to the abasic position even without irradiation,<sup>[3]</sup> it would interfere with our future studies of the photoinduced DNA damage.

## Results and Discussion

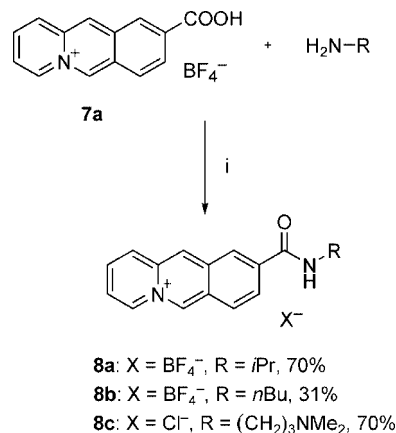
### Synthesis

The *N*-substituted carboxamidoacrididinium were prepared from the known 9-carboxyacrididinium (**7a**)<sup>[10]</sup> and the previously unknown 3-carboxyacrididinium (**7b**) tetrafluoroborates. The latter was synthesized from commercially available methyl 6-methylnicotinate (**4**), which was oxidized with selenium dioxide to methyl 6-formylnicotinate and subsequently protected as acetal **5** (Scheme 1). The quaternization with benzyl bromide, followed by the acid-induced cyclodehydration of the salt **6** gave the acid **7b**, which was further converted into its tetrafluoroborate salt by ion metathesis.



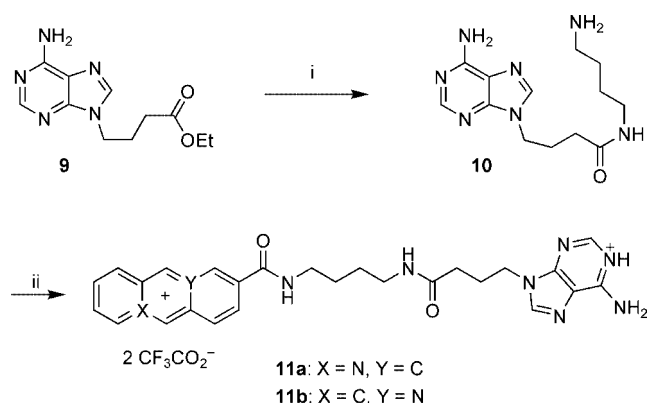
Scheme 1. Synthesis of 3-carboxyacrididinium tetrafluoroborate (**7b**). Reagents and conditions: (i) SeO<sub>2</sub>, 1,4-dioxane/water, 65 °C, 1 h; (ii) HO(CH<sub>2</sub>)<sub>2</sub>OH, *p*TsOH, toluene, reflux, 20 h, 36%; (iii) PhCH<sub>2</sub>Br, DMSO, room temp., 13 d, 54%; (iv) aqueous HBr, reflux, 20 h, 90%; (v) aqueous HBF<sub>4</sub>, 77%.

To find appropriate conditions for the amide synthesis, coupling reactions of the **7a** with selected amines were conducted (Scheme 2). Notably, the amidation of this acid by several methods, such as coupling with dicyclohexylcarbodiimide (DCC) or *N,N'*-carbonyldiimidazole (CDI)<sup>[11]</sup> led to decomposition of the acrididinium core due to the nucleophilic addition of the amines to position 6 of the acrididinium ion, and no amide could be isolated. In contrast, the corresponding amides were prepared in good yields by the mixed-anhydride method (Scheme 2). Thus, the treatment of **7a** with isobutyl chloroformate in acetonitrile in the presence of a mild base (*N*-methylmorpholine) afforded a salt of the mixed anhydride, which was allowed to react with selected amines in situ, to give the amides **8a–d**. The use of stronger bases, such as *N*-ethyl-diisopropylamine ("Hünig's base") or *N*-ethylpiperidine, led to the formation of large amounts of decomposition products. The crude amides were subjected to ion exchange and isolated as tetrafluoroborates **8a,b** or as the chloride/hydrogen chloride salt **8c**.



Scheme 2. Synthesis of 9-carboxamidoacrididinium salts. Reagents and conditions: (i) NMM, *i*BuOCOC<sub>2</sub>H<sub>5</sub>, MeCN, −20 °C to room temp., 18 h.

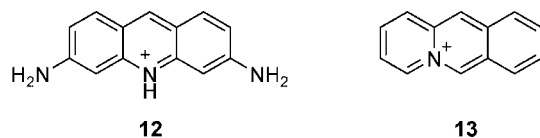
Since strong bases interfere with the synthesis of carbox-amidoacridizinium salts, preparation of conjugates **11a** and **11b** started from the attachment of a linker to the adenine residue, with coupling to the acridizinium cation in the last step (Scheme 3). Thus, ethyl 4-(adenin-9-yl)butyrate (**9**)<sup>[12]</sup> was treated with an excess of 1,4-diaminobutane in refluxing 1-propanol or in ethylene glycol at 100 °C to give the amide **10**, which was subsequently allowed to react with the isomeric acridizinium carboxylic acids **7a** or **7b** under the conditions optimized for the synthesis of model amides **8a–b**. In this case, the reaction was performed in anhydrous DMF because of the low solubility of the intermediate **10** in acetonitrile. The acridizinium–adenine conjugates **11a** and **11b** were purified by the reversed-phase chromatography and isolated as bis(trifluoroacetate) salts.



Scheme 3. Synthesis of the acridizinium–adenine conjugates **11a,b**. Reagents and conditions: (i) H<sub>2</sub>N(CH<sub>2</sub>)<sub>4</sub>NH<sub>2</sub>, *n*PrOH, reflux, 10 h, 86%; (ii) **7a** or **7b**, NMM, *i*BuOCOCl, DMF, −20 °C to room temp., 18 h, **11a**: 47%, **11b**: 54%.

### Association with Regularly Paired DNA

To assess whether carboxamidoacridizinium salts bind to DNA in general, the binding affinities of 9-carboxamidoacridizinium salts **8a–c** and the acridizinium–adenine conjugate **11a** to double-stranded (ds) polynucleotides were investigated by spectrophotometric titrations and by thermal denaturation studies with calf thymus DNA (ct DNA). In the latter experiments a known intercalator, namely proflavine (**12**),<sup>[13]</sup> and the parent acridizinium cation **13** were used as reference compounds.



Upon interaction with DNA, pronounced changes in the absorption spectra of derivatives **8a,b** and **11a,b** were observed (Figure 1). The intensity of the 0–0 transition bands of these derivatives decreases significantly (hypochromic effect), the long-wavelength absorption maximum is shifted

by about 5 nm to shorter wavelengths, red-shifted shoulders appear, and clear isosbestic points are conserved at any ligand/DNA ratio. Remarkably, the complete binding of the derivatives **8a,b**, and **11a** is achieved only at relatively high ligand/DNA ratio ( $r \geq 20$ ), whereas in the case of derivative **8c** saturation is achieved at a significantly smaller ligand/DNA ratio. The fitting of the binding isotherms to the neighbor-exclusion model<sup>[14]</sup> gives the values of the DNA-binding constants. Thus, acridizinium derivatives **8a** and **8b** as well as the conjugates **11a–b** bind to DNA with relatively small binding constants,  $K = (1–3) \times 10^4 \text{ M}^{-1}$  (Table 1), which are comparable to that of the parent acridizinium ion **13** ( $1.2 \times 10^4 \text{ M}^{-1}$ ).<sup>[15]</sup> At the same time, derivative **8c** has a significantly higher affinity towards ds DNA ( $K = 1.5 \times 10^5 \text{ M}^{-1}$ ).<sup>[16]</sup>

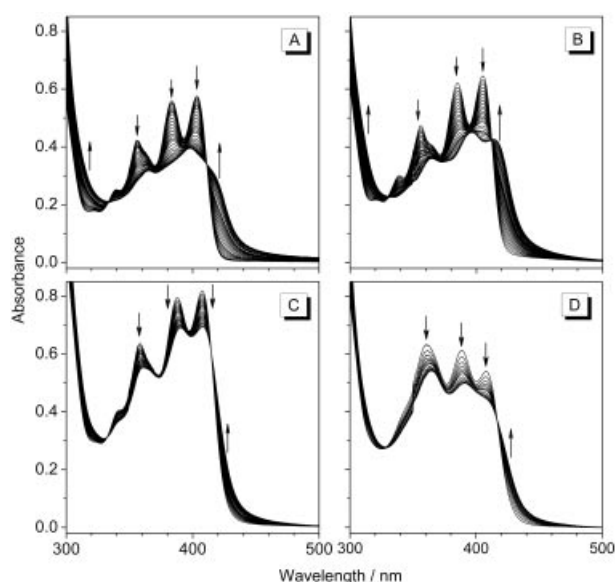


Figure 1. (A) Spectrophotometric titrations of ct DNA to compounds **8a** (A,  $c = 50 \mu\text{M}$ ), **8c** (B,  $c = 60 \mu\text{M}$ ), **11a** (C,  $c = 100 \mu\text{M}$ ) and **11b** (D,  $c = 100 \mu\text{M}$ ) in phosphate buffer. The arrows indicate the changes of the intensity of the absorption bands upon the addition of DNA (0–10 mM).

Moreover, flow linear dichroism (LD) spectroscopic studies were performed with amides **8a** and **8b** (Figure 2, A and B). Thus, in the hydrodynamic field of a rotating cuvette the DNA bases exhibit a negative LD signal at  $\lambda_{\text{max}} \approx 260 \text{ nm}$ , the intensity of which increases significantly upon the addition of compound **8a** or **8b**. This increase already shows that the interaction of **8a** or **8b** with DNA leads to a stiffening of the DNA which results in a better orientation of the macromolecule in the flow field. Moreover, upon association with DNA both acridizinium derivatives **8a** and **8b** exhibit negative LD bands in the long-wavelength range (350–450 nm, where the DNA bases do not absorb), which indicates an intercalative binding mode.<sup>[17]</sup> The reduced LD spectra ( $\text{LD}_r = \text{LD}/A$ ) of compounds **8a** and **8b** in the presence of DNA are nearly constant between 300 nm and 375 nm, thus confirming a dominant intercalative binding mode.

Table 1. Binding affinities of acridizinium derivatives **8a–c**, **11a–b**, **13** and proflavine to polymeric ds DNA, as determined from the thermal denaturation studies and spectrophotometric titrations.

Entry	Ligand	Induced $\Delta T_m$ [°C] <sup>[a]</sup> at ligand/DNA ratios $r$				$K_a \times 10^{-4}$ [M <sup>-1</sup> ] <sup>[b]</sup>
		ct DNA $r = 0.2$	ct DNA $r = 0.5$	[poly(dAdT)] <sub>2</sub> $r = 0.2$	[poly(dAdT)] <sub>2</sub> $r = 0.5$	
1	<b>8a</b>	0.4	0.5	n.d. <sup>[d]</sup>	n.d. <sup>[d]</sup>	2.1
2	<b>8b</b>	0.2	0.8	0.5	0.9	2.7
3	<b>8c</b>	7.4	11.9	8.5	15.9	15.0
4	<b>11a</b>	0.3	0.8	0.2	0.4	1.1
5	<b>11b</b>	0.6	0.7	0.2	0.9	2.9
6	<b>12</b>	10.1 <sup>[c]</sup>	15.6	18.4	24.0	n.d. <sup>[d]</sup>
7	<b>13</b>	1.2	2.6	1.6	3.5	1.2 <sup>[e]</sup>

[a] Experimental conditions:  $c_{\text{DNA}} = 40 \mu\text{M}$  DNA in BPE buffer,  $[\text{Na}^+] = 16 \text{ mM}$ ; estimated error: 0.2 °C. [b] Binding constant to ct DNA, determined by fitting the data from spectrophotometric titrations to the McGhee–von Hippel model.<sup>[14]</sup> [c] Literature value: 11.5 °C; ref.<sup>[12]</sup> [d] Not determined. [e] Ref.<sup>[15]</sup>

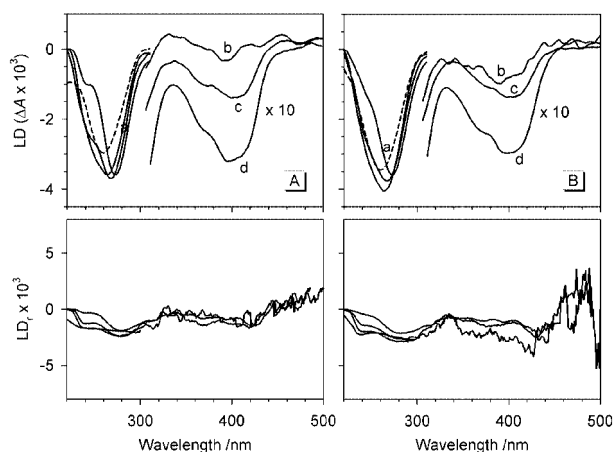


Figure 2. LD (top panels) and reduced LD (bottom panels) spectra of compounds **8a** (A) and **8b** (B) in the presence of ct DNA at ligand/DNA ratios  $r = 0$  (a), 0.04 (b), 0.08 (c), and 0.2 (d).

An additional proof for the intercalation of the carbox-amidoacridizinium salts **8b**, **8c**, and **11a** was provided by viscosimetric titrations (Figure 3). Thus, upon the addition of these derivatives to ct DNA the viscosity of the solution increases significantly, which is characteristic of DNA-intercalators,<sup>[18]</sup> as shown by comparison with proflavine (**12**). In the presence of groove binders, the viscosity of DNA solutions usually does not increase. Nevertheless, as compared to proflavine (**12**), the carboxamidoacridizinium salts **8b** and **8c** lead to a significantly smaller increase in the relative viscosity of the DNA solution, which indicates that in general the association of the acridizinium carboxamides leads to a significantly less pronounced stiffening of the DNA as compared with proflavine-DNA complexes. Presumably only a small part of the acridizinium intercalates in the binding pocket (i.e. with the long molecular axis perpendicular to the long axis of the binding pocket) such that the DNA does not need to unwind significantly to accommodate the intercalator. Notably, the addition of conjugate **11a** has only a small influence on the viscosity of the DNA solution. It may be assumed that due to the steric demand of this compound the intercalating residue occupies an even smaller area of the intercalation pocket, leading to an almost negligible change of the DNA structure.

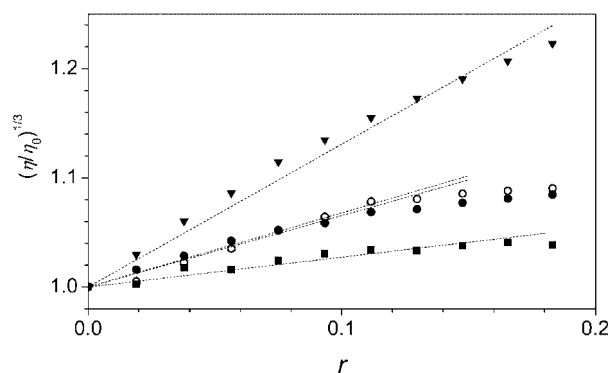


Figure 3. Viscosimetric titration of compounds **8b** (filled circles), **8c** (empty circles), **11a** (squares), and proflavine (triangles) to ct DNA (average length of 200 bp) at 25 °C.

The influence of the ligands **8a–c** and **11a** on the thermodynamic stability of ds DNA was investigated by thermal denaturation experiments (Table 1). Notably, the *N*-alkyl-substituted amides **8a** and **8b** as well as the conjugate **11a** have only a marginal effect on the stabilization of ds DNA, as indicated by a very small increase of the DNA melting temperature ( $\Delta T_m < 1$  °C; all data hereafter refer to a ligand/DNA ratio  $r$  of 0.5). This effect was much smaller than the one induced by proflavine ( $\Delta T_m = 15.6$  °C) and even the one induced by the parent compound **13** ( $\Delta T_m = 2.6$  °C). In contrast, the aminoalkyl-substituted derivative **8c** stabilizes the ds DNA significantly against thermal denaturation ( $\Delta T_m = 11.9$  °C).

Overall these results show that the carboxamidoacridizinium ligand is, in principle, a DNA intercalator as shown unambiguously by the representative flow LD spectroscopic and viscosimetric data (Figures 2 and 3). Moreover, the LD spectroscopic data demonstrate that the increasing steric demand of the *N*-terminal amide substituent does not interfere with intercalating properties, as shown by the comparison of **8a** ( $R = n\text{Bu}$ ) and **8b** ( $R = i\text{Pr}$ ). Nevertheless, the evaluation of the data from the photometric titrations reveals a low affinity of the acridizinium carboxamide ligand



to ds DNA as demonstrated by the rather low binding constants of **8a** and **8b** (Table 1), whose affinity to DNA is comparable to that of the parent compound **13**. In addition, the DNA duplex is not significantly stabilized by these intercalators, as shown by the very small increase of DNA  $T_m$  in the presence of the ligand (Table 1). Thus, other than donor substituents, such as the amino substituent,<sup>[15]</sup> the carboxamide functionality does not have a significant influence on the affinity of the acridizinium ligand towards double-stranded DNA. The DNA-binding constants of compounds **11a** and **11b** are comparable to those of **8a** and **8b** (Table 1); moreover **11a** and **11b** do not stabilize the DNA duplex, either, indicating that the introduction of the adeninyl-alkyl substituent does not have a significant impact on the interactions of the acridizinium unit with the regularly paired ds DNA. Nevertheless, it may be assumed that the  $\pi$  system of the acridizinium unit in **11a** and **11b** overlaps with the nucleic acid bases to a lesser extent than that of **8a** and **8b**. This assumption is supported by two observations: i) The hypochromic effect of the long-wavelength absorption band of **11a** and **11b** upon the addition of DNA is less pronounced than the ones observed for **8a** and **8b** (Figure 1) and ii) **11a** has a significantly smaller influence on the viscosity of DNA solutions than the acridizinium derivatives **8a** and **8b** (Figure 3), which may be explained by a significantly reduced penetration of the intercalating part into the DNA.

As compared with derivatives **8a** and **8b**, the aminoalkyl-substituted carboxamidoacridizinium salt **8c** has a significantly higher affinity towards the DNA duplex, most likely due to the attractive electrostatic interaction of the amino functionality, which is protonated in neutral aqueous solutions, with the negatively charged DNA. This assumption is in agreement with the well-known ability of the aminoalkyl substituent to enhance the binding affinity of a given ligand.<sup>[19]</sup> Moreover, in contrast to the carboxamidoacridizinium salts **8a** and **8b**, a significant stabilization of ds DNA was observed upon the addition of compound **8c** (Table 1), because the aminoalkyl substituent in compound **8c** provides a high affinity for ds DNA due to its additional cationic charge, which results in an efficient stabilization of the DNA duplex against thermal denaturation. A similar effect has been demonstrated for acridine derivatives.<sup>[20]</sup> Although the binding affinities of derivatives **8b** and **8c** are significantly different, the increase of the viscosity of a DNA solution upon the addition of these ligands is essentially the same (Figure 3). Considering that an increase in the viscosity is usually induced by an intercalator, whereas groove binders do not have an influence, it may be concluded that both compounds **8b** and **8c** intercalate into DNA, with the intercalating part (i.e. the acridizinium) having more or less the same orientation within the binding site. In the case of compound **8c** the aminoalkyl substituent is presumably accommodated in the grooves, which leads to an increase of the binding affinity and DNA stabilization (see above); however, it does not contribute to the overall change of the viscosity of the solution, which may explain the similar influence of **8b** and **8c** on the viscosity of DNA solutions.

## Interaction with Abasic Sites

The interaction of the model compounds **8a–c** and acridizinium–adenine conjugates **11a–b** with abasic-site-containing DNA structures was studied by the thermal denaturation of ds oligodeoxyribonucleotides (ODNs) in the absence or presence of these compounds (Figure 4, Table 2).

Thus, the undecamer TX was used as DNA with an abasic site, whereas the paired oligonucleotide TA was used for comparison. Because of the instability of the natural abasic sites and in accordance with established protocols, the abasic oligonucleotide (ODN3) contained a chemically stable tetrahydrofuran analogue of the deoxyribose residue. The  $T_m$  values of both oligonucleotides are slightly lower than the ones reported previously ( $T_m = 36.9^\circ\text{C}$  and  $56.0^\circ\text{C}$  for TX and TA duplexes, respectively), presumably due to irreproducible differences in the buffer composition. Notably, none of the compounds investigated, except for **8c**, had an influence on the denaturation of the fully paired TA duplex, as indicated by  $\Delta T_m$  (TA) values that lie within the experimental error range (i.e. within  $0.5^\circ\text{C}$ ). In the case of the aminoalkyl-substituted carboxamide **8c**, a small stabilizing effect is observed ( $\Delta T_m = 2.0^\circ\text{C}$  at  $r = 2.0$ ), which indicates a significant association of this compound with the TA duplex. At the same time, compounds **11a–b** show a small, but significant stabilization of the abasic site-containing TX duplex, and the observed induced shifts of the  $T_m$  increase with the increasing concentration of the ligand. Thus, the acridizinium–adenine conjugates **11a–b** show  $\Delta T_m$  values of about  $7^\circ\text{C}$  at  $r = 2.0$ , with the compound **11b** being slightly more efficient than the isomer **11a**. For comparison, the *N*-butyl-substituted derivative **8b** stabilizes the TX duplex to a lesser extent ( $\Delta T_m = 3.0^\circ\text{C}$ ). Most notably, a very efficient stabilization of the TX duplex is achieved by the compound **8c**, which shows a  $\Delta T_m$  value of  $13.3^\circ\text{C}$  at  $r = 2.0$ .

The selectivity of the ligands for the abasic site may be expressed by the  $\Delta\Delta T_m$  values [ $\Delta\Delta T_m = \Delta T_m(\text{TX}) - \Delta T_m(\text{TA})$ ] at a certain ligand concentration (Figure 5). Thus, compound **8c** has a significant preference for the DNA that contains an abasic site ( $\Delta\Delta T_m$  value of  $9.6^\circ\text{C}$  at  $r = 0.5$ ), with saturation of the binding at  $r \geq 1.0$ . The selectivity of the conjugates **11a–b** is less pronounced, and the saturation does not take place even at  $r = 2.0$ . The  $\Delta\Delta T_m$  values of these compounds, as well as those of compound **8b**, reflect a low affinity for the fully paired TA duplex.

The slightly enhanced affinity of **11a–b** to abasic DNA structures, as compared to that of the corresponding fully paired oligonucleotides, may be explained by the interaction of the adenine moiety with the unpaired thymine of the abasic DNA, which contributes to the overall DNA-binding properties of the conjugate. Nevertheless, the selectivity of conjugates **11** is relatively small compared to that of acridine–adenine conjugates such as **1** and **2**, most likely because **11a** and **11b** lack the amino groups which, in their protonated form, provide additional binding affinity by electrostatic interaction with the DNA grooves.<sup>[3]</sup> As it has

Table 2. Binding affinities of 9-carboxamidoacridizinium salts **8b–c** and conjugates **11a** and **11b** to TX and TA duplexes, as determined from the thermal denaturation studies.

$$X = \begin{array}{c} \text{5'} \\ | \\ \text{O}=\text{P}-\text{O}-\text{O}-\text{CH}_2-\text{O} \\ | \\ \text{3'} \end{array}$$

ODN1: GCG-TGT-GTG-CG  
 ODN2: CGC-ACA-CAC-GC  
 TA duplex

ODN1: GCG-TGT-GTG-CG  
 ODN3: CGC-ACX-CAC-GC  
 TX duplex

Entry	Ligand	Induced $\Delta T_m$ [°C] <sup>[a]</sup> at ligand/DNA ratios $r$ <sup>[b]</sup>			
		TX duplex		TA duplex	
		$r = 0.5$	$r = 2.0$	$r = 0.5$	$r = 2.0$
1	<b>8b</b>	1.6	3.0	0.2	0.1
2	<b>8c</b>	10.8	13.3	1.2	2.0
3	<b>11a</b>	3.4	5.9	0.5	0.2
4	<b>11b</b>	4.3	6.6	0.3	−0.3

[a] Experimental conditions:  $c_{\text{DNA}} = 5 \mu\text{M}$  in aqueous phosphate buffer,  $[\text{Na}^+] = 38.1 \text{ mM}$ ; estimated error: 0.5 °C. [b] The  $r$  values refer to the molar concentration of the oligonucleotide duplexes.

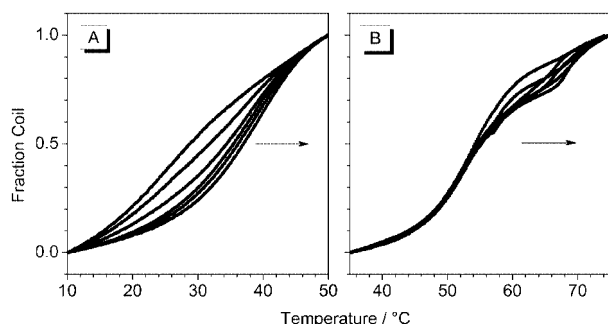


Figure 4. Thermal denaturation profiles of TX duplex (A) and TA duplex (B) ( $c_{\text{DNA}} = 5 \mu\text{M}$  in ODN buffer,  $[\text{Na}^+] = 38.1 \text{ mM}$ ) in the presence of compound **8c** at ligand/DNA ratios  $r$  of 0, 0.2, 0.5, 1.0, 1.5 and 2.0. Arrows indicate the shift of the melting curves with increasing  $r$  values.

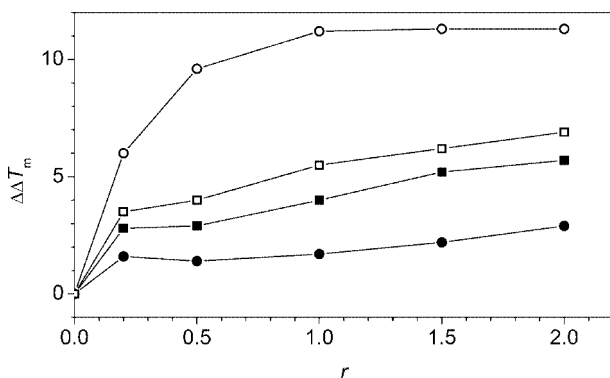


Figure 5. Plot of the  $\Delta\Delta T_m$  values for compounds **11a** (filled squares), **11b** (open squares), **8b** (filled circles) and **8c** (open circles) vs. ligand/DNA ratio  $r$ .

been shown already that adenine may be generally used as a connection point to abasic sites, and we showed in this study that the carboxamidoacridizinium salt intercalates into DNA, it may be concluded that the linker between these two units does not fit well between the abasic site and the intercalation site of the acridizinium and this has

a significant impact on the low selectivity. Presumably, an unfavorable conformation of the amido-alkyl linker results in steric interactions with the DNA backbone. In contrast, the most efficient stabilization of the abasic-site-containing oligonucleotide TX is achieved by compound **8c**, which carries no adenine substituent. Although this compound shows the most pronounced binding to the fully paired polynucleotides among the tested acridizinium derivatives, it exhibits a pronounced selectivity for DNA with abasic structures, which makes it comparable with the conjugates **1a–c** (e.g.  $\Delta\Delta T_m = 10.5$  °C for **1c** at  $r = 0.5$  under similar conditions).<sup>[5a]</sup>

As shown by the studies with ct DNA and [poly-(dAdT)]<sub>2</sub>, the relatively high affinity of **8c** for DNA as compared with that of **8a,b** and **11a,b** is caused by the association of the aminoalkyl substituent in the DNA groove. Moreover, the selective binding of acridizinium salt **8c** to abasic positions in DNA is in agreement with a recent report that the aminoalkyl-substituted acridine derivative **3**, which also carries no adenine moiety, has a high preference towards abasic sites in DNA. Thus, it may be proposed that, as shown for compound **3**, upon interaction with abasic oligonucleotides the intercalating acridizinium part of the ligand **8c** is located in the abasic pocket, while the positively charged aminoalkyl substituent provides an additional stabilization of the ligand–DNA complex by an association with the minor groove.

## Conclusions

The initial intention of this work was the synthesis of ligands that bind to abasic positions according to the established design of nucleic acid base–intercalator conjugates. Indeed, the corresponding acridizinium–adenine conjugates **11** exhibit a slight but significant selectivity towards AP sites. Nevertheless, the most surprising result is that the derivative **8c**, which was initially synthesized for comparison purposes, has the highest selectivity towards AP sites of all the compounds tested in this series. Considering similar re-

sults with the acridine derivative **3**,<sup>[7]</sup> it may be proposed that, complementary to the intercalator–nucleic acid base conjugates, aminoalkyl-substituted intercalators may be employed as promising platforms for the design of ligands that bind selectively to abasic sites. That is, the recognition of an abasic pocket may be achieved not only by nucleic acid bases or base analogues, but also by intercalators which have an appropriate geometrical shape and  $\pi$ -stacking properties. This approach may offer advantages considering the synthetic difficulties when handling nucleobases, as their functionalization of nucleic acid bases by the reaction with electrophiles is often unselective, and the nucleic-base residues may cause the conjugates to be poorly soluble. Moreover, another drawback of intercalator–nucleobase conjugates, such as **1a–d** and **11a–b** that should be considered is the competition between the intercalator moiety and the nucleic acid base for occupation of the abasic site, which may limit the abasic-site selectivity of such conjugates.

## Experimental Section

**Materials and General Instrumentations:** All commercially available chemicals were reagent-grade and used without further purification. The melting points are uncorrected. Mass spectra (ESI in positive-ion mode) were recorded at a source voltage of 6 kV. NMR spectra were measured with a Bruker Avance 400 (<sup>1</sup>H: 400 MHz, <sup>13</sup>C: 100 MHz) spectrometer; chemical shifts are given in ppm ( $\delta$ ) versus an internal standard, TMS. Unambiguous proton NMR assignments were established by means of <sup>1</sup>H–<sup>1</sup>H COSY experiments (data not given). TLC was performed with RP-18 silica gel sheets (Macherey–Nagel Alugram RP-18W/UV<sub>254</sub>) with an eluent of 1 M aqueous HCl/MeCN (80:20).

**Methyl 6-(1,3-Dioxolan-2-yl)nicotinate (5):**<sup>[21]</sup> Selenium dioxide (freshly sublimed from HNO<sub>3</sub>, 2.32 g, 20.9 mmol) dissolved in 1,4-dioxane/water (6:1, 14 mL) was added dropwise over 30 min to a stirred at 60–65 °C solution of methyl 6-methylnicotinate (**4**, 3.14 g, 20.8 mmol) in 1,4-dioxane (6 mL). After completion of the addition, the reaction mixture was stirred at 60–65 °C for 1 h, cooled to room temperature, and filtered through a pad of Celite. The filtrate was evaporated to dryness, dissolved in toluene (40 mL), and ethylene glycol (2.30 mL, 2.59 g, 41.8 mmol) was added, followed by *p*-toluenesulfonic acid monohydrate (1.19 g, 6.26 mmol). The reaction mixture was heated at reflux with a Dean–Stark water separator for 20 h, cooled to room temperature and poured into saturated aqueous Na<sub>2</sub>CO<sub>3</sub> (50 mL). After separation of the organic layer, the aqueous layer was extracted with toluene (3 × 20 mL). The combined organic layers were washed with water (20 mL), dried with anhydrous Na<sub>2</sub>SO<sub>4</sub>, and the solvent was removed in vacuo. The residue was purified by flash chromatography (SiO<sub>2</sub>; eluent: CH<sub>2</sub>Cl<sub>2</sub>/MeOH, 98:2). After evaporation of the solvents in vacuo, ester **5** (1.56 g, 36% yield) was obtained as a pale yellow low-melting solid. <sup>1</sup>H NMR (400 MHz, CDCl<sub>3</sub>):  $\delta$  = 3.95 (s, 3 H, CH<sub>3</sub>), 4.11–4.16 (m, 4 H, OCH<sub>2</sub>), 5.90 [s, 1 H, CH–(OCH<sub>2</sub>)<sub>2</sub>], 7.62 (d, <sup>3</sup>*J* = 8 Hz, 1 H, 5-H), 8.33 (dd, <sup>3</sup>*J* = 8, <sup>4</sup>*J* = 2 Hz, 1 H, 4-H), 9.21 (d, <sup>4</sup>*J* = 2 Hz, 1 H, 2-H) ppm.

**1-Benzyl-2-(1,3-dioxolan-2-yl)-5-(methoxycarbonyl)pyridinium Bromide (6):** A solution of the ester **5** (1.05 g, 5.00 mmol) and benzyl bromide (1.28 g, 0.89 mL, 7.50 mmol) in anhydrous DMSO (2 mL) was stirred under an argon atmosphere for 13 d and then poured

into AcOEt (50 mL). The white precipitate was collected, washed with acetone (2 × 10 mL) and Et<sub>2</sub>O (2 × 10 mL), and dried in vacuo over P<sub>2</sub>O<sub>5</sub>, to give 1.02 g (54% yield) of salt **6** as a white amorphous solid. Crystallization from EtOH/AcOEt afforded fine colorless needles; m.p. 134–136 °C. <sup>1</sup>H NMR (400 MHz, CD<sub>3</sub>OD):  $\delta$  = 4.01 (s, 3 H, CH<sub>3</sub>), 4.21 (s, 4 H, CH<sub>2</sub>CH<sub>2</sub>), 6.14 (s, 2 H, CH<sub>2</sub>N<sup>+</sup>), 7.40–7.50 (m, 5 H, Ar-H), 8.52 (d, <sup>3</sup>*J* = 8 Hz, 1 H, 5-H), 9.12 (dd, <sup>3</sup>*J* = 8, <sup>4</sup>*J* = 2 Hz, 1 H, 4-H), 9.39 (d, <sup>4</sup>*J* = 2 Hz, 1 H, 2-H) ppm. <sup>13</sup>C NMR (100 MHz, CD<sub>3</sub>OD):  $\delta$  = 54.2 (CH<sub>3</sub>), 62.8 (CH<sub>2</sub>N<sup>+</sup>), 67.5 (2 C, CH<sub>2</sub>CH<sub>2</sub>), 98.9 (CH), 127.8 (CH), 129.9 (CH), 130.8 (CH), 131.0 (CH), 132.3 (C<sub>q</sub>), 133.7 (C<sub>q</sub>), 147.9 (CH), 148.9 (CH), 162.9 (CO) ppm. C<sub>17</sub>H<sub>18</sub>BrNO<sub>4</sub> (380.2): calcd. C 53.70, H 4.77, N 3.68; found C 54.17, H 4.81, N 3.68.

**3-Carboxyacridizinium Bromide (7b):** A solution of the salt **6** (0.87 g, 2.30 mmol) in aqueous HBr (48%, 10 mL) was heated at reflux for 20 h. After this time, 3 mL of HBr were distilled off, the residue was cooled to room temperature and THF (40 mL) was added. The yellow precipitate was collected, washed with THF (2 × 10 mL) and Et<sub>2</sub>O (2 × 10 mL), and dried in vacuo over P<sub>2</sub>O<sub>5</sub>, to give 0.63 g (90% yield) of **7b** as a yellow crystalline solid; m.p. 265–270 °C (EtOH/H<sub>2</sub>O) (dec.). <sup>1</sup>H NMR (400 MHz, [D<sub>6</sub>]DMSO):  $\delta$  = 8.08 (dd, <sup>3</sup>*J* = 8, <sup>3</sup>*J* = 8 Hz, 1 H, 8-H), 8.23 (dd, <sup>3</sup>*J* = 7, <sup>3</sup>*J* = 9 Hz, 1 H, 9-H), 8.32 (dd, <sup>3</sup>*J* = 9, <sup>4</sup>*J* = 2 Hz, 1 H, 2-H), 8.46 (d, <sup>3</sup>*J* = 9 Hz, 1 H, 10-H), 8.51 (d, <sup>3</sup>*J* = 8 Hz, 1 H, 7-H), 8.64 (d, <sup>3</sup>*J* = 9 Hz, 1 H, 1-H), 9.35 (s, 1 H, 11-H), 9.94 (s, 1 H, 4-H), 10.74 (s, 1 H, 6-H), 14.43 (br. s, 1 H, COOH) ppm. <sup>13</sup>C NMR (400 MHz, [D<sub>6</sub>]DMSO):  $\delta$  = 124.7 (CH, C11); 125.0 (C<sub>q</sub>); 125.9 (C<sub>q</sub>); 127.1 (CH, C1); 127.3 (CH, C10); 128.5 (CH, C7); 128.9 (CH, C2); 131.4 (CH, C8); 135.7 (CH, C9); 136.2 (C<sub>q</sub>); 137.5 (CH, C4); 137.8 (C<sub>q</sub>); 142.3 (CH, C6); 164.1 (COOH) ppm. MS (ESI<sup>+</sup>): *m/z* (%) = 224 (100) [M]<sup>+</sup>, 447 (80) [2 M – H]<sup>+</sup>, 670 (42) [3 M – 2 H]<sup>+</sup>.

**General Procedure for the Conversion of Carboxyacridizinium Bromides into Tetrafluoroborates:** The salts **7a–b** (0.480 g, 1.58 mmol) were dissolved in boiling water (10 mL) and treated with aqueous HBF<sub>4</sub> (50%, 2 mL). After the mixture was slowly cooled to room temperature, the tetrafluoroborate separated as a yellow crystalline precipitate, which was collected, washed with cold water, and dried in vacuo over P<sub>2</sub>O<sub>5</sub>.

**9-Carboxyacridizinium Tetrafluoroborate (7a):** Yield 98%, bright yellow needles, m.p. (dec.) 236–240 °C; C<sub>14</sub>H<sub>10</sub>BF<sub>4</sub>NO<sub>2</sub> (311.0): calcd. C 54.06, H 3.24, N 4.50; found C 54.01, H 3.14, N 4.47.

**3-Carboxyacridizinium Tetrafluoroborate (7b):** Yield 77%, lemon-yellow needles, m.p. (dec.) 240–244 °C; C<sub>14</sub>H<sub>10</sub>BF<sub>4</sub>NO<sub>2</sub> (311.0): calcd. C 54.06, H 3.24, N 4.50; found C 54.18, H 3.38, N 4.51.

**General Procedure for the Synthesis of 9-Carboxamidoacridizinium Salts:** To a warm (50–60 °C) solution of the salt **7a** (0.62 g, 2.0 mmol) in MeCN (30 mL), *N*-methylmorpholine (0.24 mL, 0.22 g, 2.2 mmol) was added; a yellow precipitate was observed. The suspension was cooled to –20 °C under an argon atmosphere and treated with isobutyl chloroformate (0.29 mL, 0.30 g, 2.2 mmol). The reaction mixture was stirred at this temperature for 10 min, and the precipitate slowly dissolved. The amine (2.0 mmol) was added dropwise under vigorous stirring. The reaction mixture was stirred for 2 h at –20 °C and warmed to room temperature during 18 h. The suspension was evaporated to dryness; the residue was dissolved in ca. 15 mL of warm (50–60 °C) water and treated with a concentrated aqueous solution of NaBF<sub>4</sub> (2.0 g, 18 mmol). The yellow precipitate was collected, washed with water (2 × 5 mL) and Et<sub>2</sub>O (2 × 10 mL) and dried in vacuo over P<sub>2</sub>O<sub>5</sub>. Further purification was achieved by column chromatography (neutral alumina, activity grade I, eluent: CHCl<sub>3</sub>/MeOH/AcOH, 90:10:1), followed



by evaporation of the solvent and crystallization of the residue from MeCN/AcOEt.

**9-(*N*-Isopropylcarboxamido)acridizinium Tetrafluoroborate (8a):** Yield 0.49 g (70%); fine pale yellow needles;  $R_f = 0.18$ .  $^1\text{H}$  NMR (400 MHz,  $[\text{D}_6]\text{DMSO}$ ):  $\delta = 1.26$  (d,  $^3J = 7$  Hz, 6 H,  $\text{CH}_3$ ), 4.21 (m,  $^3J = 7$  Hz, 1 H,  $\text{CHMe}_2$ ), 8.03 (app. t,  $^3J = 7$  Hz, 1 H, 3-H), 8.15 (dd,  $^3J = 9$ ,  $^3J = 7$  Hz, 1 H, 2-H), 8.29 (d,  $^3J = 9$ ,  $^4J = 1$  Hz, 1 H, 8-H), 8.53 (d,  $^3J = 9$  Hz, 1 H, 7-H), 8.66 (d,  $^3J = 9$  Hz, 1 H, 1-H), 8.80 (s, 1 H, 10-H), 8.90 (d,  $^3J = 8$  Hz, 1 H, NH), 9.34–9.38 (m, 2 H, 11-H, 4-H), 10.52 (s, 1 H, 6-H) ppm.  $^{13}\text{C}$  NMR (100 MHz,  $[\text{D}_6]\text{DMSO}$ ):  $\delta = 22.3$  ( $2\text{CH}_3$ ), 41.7 (CH), 122.9 (CH), 126.1 (CH), 126.2 ( $\text{C}_q$ ), 126.5 (CH), 127.1 (CH), 128.4 (CH), 129.1 (CH), 131.6 (CH), 134.6 (CH), 134.8 ( $\text{C}_q$ ), 137.9 ( $\text{C}_q$ ), 139.2 ( $\text{C}_q$ ), 140.2 (CH), 164.1 (CO) ppm. IR (KBr):  $\tilde{\nu} = 1546$  (amide II), 1653 s (amide I)  $\text{cm}^{-1}$ . **Chloride:** Fine yellow needles, m.p. 230–235 °C.  $\text{C}_{17}\text{H}_{17}\text{ClN}_2\text{O}\cdot\text{H}_2\text{O}$ : calcd. C 64.05, H 6.01, N 8.79; found C 63.91, H 5.91, N 8.81.

**9-(*N*-Butylcarboxamido)acridizinium Tetrafluoroborate (8b):** Yield 0.23 g (31%); fine pale yellow needles, m.p. 131–133 °C;  $R_f = 0.11$ .  $^1\text{H}$  NMR (400 MHz,  $[\text{D}_6]\text{DMSO}$ ):  $\delta = 0.95$  (t,  $^3J = 7$  Hz, 3 H,  $\text{CH}_3$ ), 1.40 (m, 2 H,  $\text{CH}_2$ ), 1.59 (quint,  $^3J = 7$  Hz, 2 H,  $\text{CH}_2$ ), 3.37 (m, overlap with  $\text{H}_2\text{O}$ ,  $\text{CH}_2\text{NH}$ ), 8.03 (app. t,  $^3J = 7$  Hz, 1 H, 3-H), 8.15 (dd,  $^3J = 9$ ,  $^3J = 7$  Hz, 1 H, 2-H), 8.29 (d,  $^3J = 9$  Hz, 1 H, 8-H), 8.54 (d,  $^3J = 9$  Hz, 1 H, 7-H), 8.66 (d,  $^3J = 9$  Hz, 1 H, 1-H), 8.79 (s, 1 H, 10-H), 9.09 (t,  $^3J = 5$  Hz, 1 H, NH), 9.35–9.37 (m, 2 H, 11-H, 4-H), 10.51 (s, 1 H, 6-H) ppm.  $^{13}\text{C}$  NMR (100 MHz,  $[\text{D}_6]\text{DMSO}$ ):  $\delta = 13.6$  ( $\text{CH}_3$ ), 19.6 ( $\text{CH}_2$ ), 31.0 ( $\text{CH}_2$ ), 39.0 ( $\text{CH}_2$ ), 122.8 (CH), 125.9 (CH), 126.0 ( $\text{C}_q$ ), 126.2 (CH), 126.9 (CH), 128.4 (CH), 128.8 (CH), 131.5 (CH), 134.4 (CH), 134.7 ( $\text{C}_q$ ), 137.8 ( $\text{C}_q$ ), 139.0 ( $\text{C}_q$ ), 140.0 (CH), 164.7 (CO) ppm. MS ( $\text{ESI}^+$ ):  $m/z$  (%) = 279 (100)  $[\text{M}]^+$ , 645 (5)  $[2\text{M} + \text{BF}_4]^+$ .  $\text{C}_{18}\text{H}_{19}\text{BF}_4\text{N}_2\text{O}\cdot\frac{1}{4}\text{H}_2\text{O}$  (370.7): calcd. C 58.33, H 5.30, N 7.56; found C 58.21, H 5.18, N 7.56.

**9-[*N*-3-(Dimethylamino)propyl]carboxamido]acridizinium Chloride (8c):** To a warm (50–60 °C) solution of the  $\text{BF}_4^-$  salt **7a** (933 mg, 3.00 mmol) in MeCN (45 mL), *N*-methylmorpholine (363  $\mu\text{L}$ , 3.33 mmol) was added, and a yellow precipitate has separated. The suspension was cooled to –10 °C under an argon atmosphere and treated with isobutyl chloroformate (429  $\mu\text{L}$ , 451 mg, 3.30 mmol). The reaction mixture was stirred at this temperature for 15 min, and the precipitate slowly dissolved. 1,3-Bis(dimethylamino)propane (413  $\mu\text{L}$ , 337 mg, 3.30 mmol) and pyridine hydrochloride (381 mg, 3.30 mmol) in anhydrous DMF (10 mL) were added dropwise over 10 min under vigorous stirring. The reaction mixture was stirred for 2 h at –10 °C and warmed to room temperature during 18 h. The yellow hygroscopic precipitate was collected, washed with MeCN (5 mL) and  $\text{Et}_2\text{O}$  ( $2 \times 5$  mL), dissolved in MeOH (5 mL) and passed through an ion-exchange column (Dowex 1X8 in the chloride form). After an additional filtration and removal of the solvent in vacuo, the residue was recrystallized from *i*PrOH/MeOH, to give 0.80 g (70% yield) of **8c** as dirty-yellow amorphous solid, m.p. (dec.) 248–249 °C;  $R_f = 0.33$ .  $^1\text{H}$  NMR (400 MHz,  $\text{CD}_3\text{OD}$ ):  $\delta = 2.15$  (dt,  $^3J = 7$ ,  $^3J = 7$  Hz, 2 H,  $\text{CH}_2\text{CH}_2\text{CH}_2$ ), 2.96 (s, 6 H,  $\text{CH}_3$ ), 3.31 (m, overlap with  $\text{CD}_3\text{OD}$ ,  $\text{CH}_2\text{NH}$ ), 3.61 (t,  $^3J = 7$  Hz, 2 H,  $\text{CH}_2\text{NMe}_2$ ), 7.98 (d,  $^3J = 7$  Hz, 1 H, 3-H), 8.13 (dd,  $^3J = 9$ ,  $^3J = 7$  Hz, 1 H, 2-H), 8.32 (d,  $^3J = 9$  Hz, 1 H, 8-H), 8.53 (d,  $^3J = 9$  Hz, 1 H, 7-H), 8.60 (d,  $^3J = 9$  Hz, 1 H, 1-H), 8.87 (s, 1 H, 10-H), 9.30–9.32 (m, 2 H, 11-H, 4-H), 10.36 (s, 1 H, 6-H) ppm.  $^{13}\text{C}$  NMR (100 MHz,  $\text{CD}_3\text{OD}$ ):  $\delta = 26.0$  ( $\text{CH}_2$ ), 38.0 ( $\text{CH}_2$ ), 43.6 ( $2\text{CH}_3$ ), 56.8 ( $\text{CH}_2$ ), 124.4 (CH), 127.9 (CH), 128.0 (CH), 128.4 ( $\text{C}_q$ ), 128.5 (CH), 129.7 (CH), 130.3 (CH), 132.9 (CH), 135.6 (CH), 136.9 ( $\text{C}_q$ ), 139.9 ( $\text{C}_q$ ), 140.4 ( $\text{C}_q$ ), 141.0 (CH), 168.4

(CO) ppm. MS ( $\text{ESI}^+$ ):  $m/z$  (%) = 308 (100)  $[\text{M}]^+$ , 651 (5)  $[2\text{M} + \text{Cl}]^+$ .  $\text{C}_{19}\text{H}_{22}\text{ClN}_3\text{O}\cdot\frac{1}{2}\text{HCl}$  (362.1): calcd. C 63.03, H 6.26, N 11.61; found C 63.30, H 6.16, N 11.43.

***N*-(4-Aminobutyl)-4-(adenin-9-yl)butyramide (10):** A solution of the ester **9**<sup>[22]</sup> (1.00 g, 4.00 mmol) and 1,4-diaminobutane (2.82 g, 32.0 mmol) in *n*PrOH (8 mL) was heated at reflux for 10 h, and the reaction was monitored by TLC. After the evaporation of all volatile components in vacuo, the residue was triturated with  $\text{Et}_2\text{O}$  (15 mL), the solid was collected, washed with  $\text{Et}_2\text{O}$  (5 mL) and MeCN ( $2 \times 5$  mL) and dried in vacuo over KOH, to give **10** (1.00 g, 86% yield) as a white hygroscopic amorphous solid, which was used without further purification;  $R_f = 0.79$ .  $^1\text{H}$  NMR (400 MHz,  $\text{CD}_3\text{OD}$ ):  $\delta = 1.45$ – $1.50$  (m, 4 H,  $\text{CH}_2$ ), 2.16–2.21 (m, 4 H,  $\text{CH}_2$ ), 2.64 (t,  $^3J = 7$  Hz, 2 H,  $\text{CH}_2\text{NH}_2$ ), 3.12 (t,  $^3J = 7$  Hz, 2 H,  $\text{CH}_2\text{NHCO}$ ), 4.28 (t,  $^3J = 7$  Hz, 2 H,  $\text{CH}_2$ -Ade), 8.13 (s, 1 H, Ade-H), 8.21 (s, 1 H, Ade-H) ppm.  $^{13}\text{C}$  NMR (100 MHz,  $\text{CD}_3\text{OD}$ ):  $\delta = 27.2$  ( $\text{CH}_2$ ), 27.7 ( $\text{CH}_2$ ), 30.9 ( $\text{CH}_2$ ), 33.8 ( $\text{CH}_2$ ), 40.2 ( $\text{CH}_2$ ), 42.1 ( $\text{CH}_2$ ), 44.4 ( $\text{CH}_2$ ), 120.0 ( $\text{C}_q$ , C5), 142.8 (CH, C8), 150.8 ( $\text{C}_q$ , C4), 153.7 (CH, C2), 157.3 ( $\text{C}_q$ , C6), 174.4 (CO) ppm. MS ( $\text{ESI}^+$ ):  $m/z$  (%) = 147 (28)  $[\text{M} + 2\text{H}]^{2+}$ , 292 (100)  $[\text{M} + \text{H}]^+$ . **Dipicrate:** M.p. 200–202 °C (EtOH).  $\text{C}_{13}\text{H}_{21}\text{N}_7\text{O}\cdot 2\text{C}_6\text{H}_3\text{N}_3\text{O}_7$  (749.6): calcd. C 40.06, H 3.63, N 24.29; found C 40.00, H 3.55, N 23.88.

**General Procedure for the Synthesis of Acridizinium–Adenine Conjugates:** Carboxyacridizinium tetrafluoroborate **7a** or **7b** (311 mg, 1.00 mmol) was dissolved in anhydrous DMF (10 mL) and treated with *N*-methylmorpholine (121  $\mu\text{L}$ , 110 mg, 1.10 mmol). The solution was cooled to –25 °C under an argon atmosphere and treated with isobutyl chloroformate (143  $\mu\text{L}$ , 150 mg, 1.10 mmol). After stirring for 10 min at this temperature, amine **10** (0.350 g, 1.20 mmol), dissolved in anhydrous DMF (15 mL), was added dropwise over 10 min. The reaction mixture was stirred at –25 °C for 2 h and warmed to room temperature during 18 h. Hydrogen chloride (2.5 mL of a 1 M solution in  $\text{Et}_2\text{O}$ , 2.5 mmol) was added and, after stirring for 30 min at room temperature, the reaction mixture was evaporated to a final volume of about 2 mL. The residue was triturated with MeCN (25 mL), and the pale yellow precipitate was collected, washed with MeCN ( $3 \times 10$  mL) and AcOEt ( $2 \times 10$  mL) and dried in vacuo over  $\text{P}_2\text{O}_5$ , yielding the crude dichloride salt. A portion of the product was purified by MPLC (RP-18; eluent: 1% aqueous TFA/MeCN, 85:15). The eluate was evaporated to dryness, and the residue was recrystallized from MeOH/AcOEt, to give analytically pure bis(trifluoroacetate) salt.

**9-[*N*-{4-[4-(Adenin-9-yl)butyrylamino]butyl}carboxamido]acridizinium Trifluoroacetate Hydrogen Trifluoroacetate (11a):** Yield of the crude salt: 270 mg (47% yield). Purified sample: lemon-yellow microcrystalline solid; m.p. (dec.) 181–184 °C (MeOH/AcOEt);  $R_f = 0.24$ .  $^1\text{H}$  NMR (400 MHz,  $\text{CD}_3\text{OD}$ ):  $\delta = 1.57$ – $1.64$  (m, 2 H, Acr-CONH- $\text{CH}_2\text{CH}_2\text{CH}_2\text{CH}_2\text{NH}$ ), 1.68– $1.75$  (m, 2 H, Acr-CONH- $\text{CH}_2\text{CH}_2\text{CH}_2$ ), 2.19– $2.29$  (m, 4 H, Ade- $\text{CH}_2\text{CH}_2\text{CH}_2\text{CO}$ ), 3.21 (t,  $^3J = 7$  Hz, 2 H, Acr-CONH- $\text{CH}_2\text{CH}_2\text{CH}_2\text{CH}_2\text{NH}$ ), 3.50 (t,  $^3J = 7$  Hz, 2 H, Acr-CONH- $\text{CH}_2$ ), 4.35 (t,  $^3J = 7$  Hz, 2 H, Ade- $\text{CH}_2$ ), 7.97 (dd,  $^3J = 7$ ,  $^3J = 8$  Hz, 1 H, 3-H), 8.12 (dd,  $^3J = 8$  Hz, 1 H, 2-H), 8.27 (dd,  $^3J = 9$ ,  $^4J = 1$  Hz, 1 H, 8-H), 8.33 (s, 1 H, Ade-H), 8.37 (s, 1 H, Ade-H), 8.50 (d,  $^3J = 9$  Hz, 1 H, 7-H), 8.58 (d,  $^3J = 9$  Hz, 1 H, 1-H), 8.74 (s, 1 H, 10-H), 9.23 (s, 1 H, 11-H), 9.27 (d,  $^3J = 7$  Hz, 1 H, 4-H), 10.31 (s, 1 H, 6-H) ppm.  $^{13}\text{C}$  NMR (100 MHz,  $\text{CD}_3\text{OD}$ ):  $\delta = 27.0$  ( $\text{CH}_2$ ), 27.8 ( $\text{CH}_2$ ), 27.9 ( $\text{CH}_2$ ), 33.7 ( $\text{CH}_2$ ), 40.1 ( $\text{CH}_2$ ), 41.1 ( $\text{CH}_2$ ), 45.0 ( $\text{CH}_2$ ), 119.8 ( $\text{C}_q$ ), 124.4 (CH), 127.7 (CH), 127.8 (CH), 128.4 (CH), 128.5 ( $\text{C}_q$ ), 129.7 (CH), 130.3 (CH), 132.9 (CH), 135.6 (CH), 137.0 ( $\text{C}_q$ ), 140.0 ( $\text{C}_q$ ), 141.0 (CH), 141.1 ( $\text{C}_q$ ), 145.4 (CH), 145.6 (CH), 150.5 ( $\text{C}_q$ ), 152.0 ( $\text{C}_q$ ), 167.9 (CO), 174.4 (CO) ppm. MS



(ESI<sup>+</sup>): *m/z* (%) = 498 (100) [M]<sup>+</sup>. C<sub>31</sub>H<sub>30</sub>F<sub>6</sub>N<sub>8</sub>O<sub>6</sub> (724.6): calcd. C 51.38, H 4.17, N 15.46; found C 51.05, H 4.13, N 15.16.

**3-[N-{4-[4-(Adenin-9-yl)butylamino]butyl}carboxamido]-acridizinium Trifluoroacetate Hydrogen Trifluoroacetate (11b):** Yield of the crude dichloride: 305 mg (54%). Purified sample: lemon-yellow prisms; m.p. 88–90 °C; *R*<sub>f</sub> = 0.21. <sup>1</sup>H NMR (400 MHz, CD<sub>3</sub>OD): δ = 1.57–1.64 (m, 2 H, Acr-CONH-CH<sub>2</sub>CH<sub>2</sub>CH<sub>2</sub>CH<sub>2</sub>NH); 1.68–1.75 (m, 2 H, Acr-CONH-CH<sub>2</sub>CH<sub>2</sub>CH<sub>2</sub>), 2.18–2.28 (m, 4 H, Ade-CH<sub>2</sub>CH<sub>2</sub>CH<sub>2</sub>CO), 3.20 (t, <sup>3</sup>*J* = 7 Hz, 2 H, Acr-CONH-CH<sub>2</sub>CH<sub>2</sub>CH<sub>2</sub>CH<sub>2</sub>NH), 3.51 (t, <sup>3</sup>*J* = 7 Hz, 2 H, Acr-CONH-CH<sub>2</sub>), 4.33 (t, <sup>3</sup>*J* = 7 Hz, 2 H, Ade-CH<sub>2</sub>), 8.06 (dd, <sup>3</sup>*J* = 7, <sup>3</sup>*J* = 9 Hz, 1 H, 8-H), 8.19 (dd, <sup>3</sup>*J* = 7, <sup>3</sup>*J* = 9 Hz, 1 H, 9-H), 8.27 (s, 1 H, Ade-H), 8.29–8.31 (m, 2 H, 2-H, Ade-H), 8.41 (d, <sup>3</sup>*J* = 9 Hz, 1 H, 10-H), 8.50 (d, <sup>3</sup>*J* = 9 Hz, 1 H, 7-H), 8.55 (d, <sup>3</sup>*J* = 9 Hz, 1 H, 1-H), 9.17 (s, 1 H, 11-H), 9.67 (s, 1 H, 4-H), 10.37 (s, 1 H, 6-H) ppm. <sup>13</sup>C NMR (100 MHz, CD<sub>3</sub>OD): δ = 27.1 (CH<sub>2</sub>), 27.6 (CH<sub>2</sub>), 27.9 (CH<sub>2</sub>), 33.7 (CH<sub>2</sub>), 40.1 (CH<sub>2</sub>), 41.2 (CH<sub>2</sub>), 44.8 (CH<sub>2</sub>), 111.9 (C<sub>q</sub>), 126.3 (CH), 128.2 (CH), 128.5 (CH), 129.5 (CH), 129.6 (CH), 130.6 (C<sub>q</sub>), 132.9 (CH), 136.0 (CH), 136.9 (CH), 138.2 (C<sub>q</sub>), 138.3 (C<sub>q</sub>), 139.3 (C<sub>q</sub>), 142.5 (CH), 144.6 (CH), 148.2 (CH), 150.6 (C<sub>q</sub>), 153.8 (C<sub>q</sub>), 164.6 (CO), 174.4 (CO) ppm. C<sub>31</sub>H<sub>30</sub>F<sub>6</sub>N<sub>8</sub>O<sub>6</sub> (724.6): calcd. C 51.38, H 4.17, N 15.46; found C 51.60, H 4.30, N 15.77.

**Nucleic Acid Binding Studies:** All buffer solutions were prepared from purified water (18 MΩ cm<sup>-1</sup>) and biochemistry-grade chemicals. The buffer solutions were stored at 4 °C up to three months and filtered through a PVDF membrane filter (pore size 0.45 μm) prior to use. BPE buffer (6.0 mM Na<sub>2</sub>HPO<sub>4</sub>, 2.0 mM NaH<sub>2</sub>PO<sub>4</sub>, 1.0 mM Na<sub>2</sub>EDTA; total Na<sup>+</sup> concentration 16.0 mM; pH 7.0) was used for spectrophotometric DNA titrations and thermal denaturation studies (except for the work with synthetic oligonucleotides). ODN buffer (6.1 mM Na<sub>2</sub>HPO<sub>4</sub>, 3.9 mM NaH<sub>2</sub>PO<sub>4</sub>, 1.0 mM Na<sub>2</sub>EDTA, 20 mM NaCl; total Na<sup>+</sup> concentration 38.1 mM; pH 7.0) was used for thermal denaturation studies with synthetic oligonucleotides. ETN buffer (1 mM Na<sub>2</sub>EDTA, 10 mM TRIS, 10 mM NaCl; pH 7.0) was used for flow LD studies of DNA-ligand complexes.

Calf thymus DNA (type I; highly polymerized sodium salt; ε = 12824 cm<sup>-1</sup> M<sup>-1</sup>) was purchased from Sigma (St. Louis, MO, USA); synthetic polynucleotide [poly(dAdT)]<sub>2</sub> was purchased from Amersham Biosciences (Piscataway, NJ, USA) and used without further purification. The polynucleotides were dissolved in BPE at a concentration of 1–2 mg/mL<sup>-1</sup> and left at 4 °C overnight. After being agitated in an ultrasonic bath for 10 min, the solution was filtered through a membrane filter to remove any insoluble material. Oligodeoxyribonucleotides (synthesis scale of 200 nmol, purified by RP-HPLC) were purchased from Eurogentec S.A. (Seraing, Belgium); their quality was confirmed by mass spectrometric analysis data provided by the manufacturer. The lyophilized oligonucleotides were dissolved in ODN buffer to a strand concentration of 500 μM. Working solutions of the ligands were prepared in ODN buffer at a concentration of 200 μM by dilution of the stock solutions (1 mM in MeOH).

**Flow LD:** Spectra of DNA-ligand complexes were obtained according to the previously published procedure.<sup>[15]</sup>

**Spectrophotometric Titrations with ct DNA:** UV/Vis spectra were recorded on a double-beam spectrophotometer. Except for experiments at varying temperature, spectrophotometric measurements were performed in thermostatted quartz sample cells at 20 °C. Spectrophotometer slit widths were kept at 2 nm. Working solutions were prepared by the dilution of stock solutions (1 mM in

MeOH) with BPE buffer to a final concentration of 50 μM immediately before the experiments.

To avoid dilution of the analyte solutions, the titrant solutions contained ct DNA at a concentration of 1–2 mM (approximately 1–2 mg/mL) as well as the ligand at the same concentration as in the titrated solution. Aliquots (2.00 mL) of the analyte solutions in BPE buffer were placed into quartz spectrophotometric cells and titrated with the titrant solutions in 0.5–2 equiv. intervals, and UV/Vis spectra were recorded (wavelength range 300–600 nm). The titrations were finished after no changes were observed in the absorption spectra upon the addition of at least three 2 equiv. portions of the titrant. All spectrophotometric titrations were performed at least three times to ensure reproducibility.

Data evaluation and determination of the binding constants were performed according to published methods.<sup>[23]</sup> Thus, the concentration of the ligand bound to the DNA was calculated from Equation (1).

$$c_b = c_L \times (A_f - A) / (A_f - A_b) \quad (1)$$

*c*<sub>L</sub> is the bulk concentration of the ligand, *A*<sub>f</sub> is the absorbance at a given wavelength in the absence of DNA, *A*<sub>b</sub> is the absorbance of the fully bound ligand, and *A* is the absorbance at a given ligand/DNA ratio. The concentration of the unbound dye (*c*) was calculated from Equation (2).

$$c = c_L - c_b \quad (2)$$

The ratio of bound ligand molecules per DNA base pair (*r*) was calculated using Equation (3).

$$r = (c_b) / (c_{\text{DNA}}) \quad (3)$$

The data were presented as Scatchard plots (*r/c* vs. *r* values) and numerically fitted to the neighbor-exclusion model of McGhee and von Hippel [Equation (4)],<sup>[14]</sup> to determine the values of the binding constant (*K*) and the binding site size (*n*). The numerical fitting was performed using the Levenberg–Marquardt non-linear curve fitting algorithm as implemented in the software package Origin<sup>®</sup> 7.5.

$$r/c = K (1 - nr) \{ (1 - nr) / [1 - (n - 1)r] \}^{n-1} \quad (4)$$

**Viscosimetric Titrations:** The measurements were performed with a micro-Ubbelohde viscometer (Schott Instruments), filled with 2.5 mL of sample solution. The flow time for the BPE buffer (pH 7.0) and of the ct DNA solution (1.0 mM) under the particular conditions were determined. Subsequently, samples were prepared to give solutions with total ligand/DNA ratios from 0 to 0.2. The flow times were measured after a thermal equilibration period of 5 min. Each sample flow time was measured three times and an average value was reported. Proflavine hemisulfate (Sigma) was included in these experiments as a reference compound. The viscosity of the solution *η* in the presence of a ligand was calculated from the flow time of a sample (*t*<sub>L</sub>) subtracted by the flow time of the buffer solution (*t*<sub>0</sub>) as *η* = (*t*<sub>L</sub> - *t*<sub>0</sub>) / *t*<sub>0</sub>. The viscosity of the ct DNA solution alone was calculated as *η*<sub>0</sub> = (*t* - *t*<sub>0</sub>) / *t*<sub>0</sub>. The relative viscosity was presented as (*η*/*η*<sub>0</sub>)<sup>1/3</sup> according to the theory of Cohen and Eisenberg,<sup>[18a]</sup> and plotted as a function of the ligand/DNA ratio, *r* = *c*<sub>L</sub> / *c*<sub>DNA</sub>.<sup>[24]</sup>

**Thermal Denaturation Studies:** Aliquots of a stock solution of the ligand (1 mM in MeOH) were pipetted into Eppendorf vials and the latter were left open until all the solvent had evaporated. The residue was dissolved in BPE buffer. The volume of the buffer solution was calculated taking into account the concentration of the

stock solution of the DNA, to provide a final volume of 1.00 mL. The samples were degassed in an ultrasonic bath for 15 min. Fixed amounts of nucleic acids (final concentration of 40  $\mu\text{M}$ ) were added; the samples were mixed briefly and transferred into masked, semi-micro quartz cells (pathlength  $l = 1$  cm). In the case of the thermal denaturation experiments with oligonucleotides, the samples were prepared by mixing the two oligonucleotide strands (final concentration of each strand of 5  $\mu\text{M}$ ) with working solutions of the ligands and ODN buffer, to give a final volume of 1 mL.

DNA thermal denaturation profiles were recorded on a double-beam spectrophotometer equipped with a thermoelectric temperature controller. Samples were heated from 20.0  $^{\circ}\text{C}$  to 97.0  $^{\circ}\text{C}$  at a rate of 0.2  $\text{deg min}^{-1}$ , while the absorbance was monitored at 260 nm. In the case of the experiments with the undecamers, an additional annealing step was required (heating from ambient temperature to 80  $^{\circ}\text{C}$  at 2.5  $\text{deg min}^{-1}$ , maintaining this temperature for 5 min, and cooling to 5  $^{\circ}\text{C}$  at 1.0  $\text{deg min}^{-1}$ , followed by a heating run in which the absorption was determined). The temperatures of DNA melting transitions,  $T_{\text{m}}$ , were determined from first-derivative plots of absorbance vs. temperature. The ligand-induced shifts of DNA melting transitions,  $\Delta T_{\text{m}} = T_{\text{m}}(\text{DNA-ligand}) - T_{\text{m}}(\text{DNA})$  were plotted as a function of ligand/DNA ratio,  $r = c_{\text{L}} / c_{\text{DNA}}$ .

## Acknowledgments

Generous support by the Deutsche Forschungsgemeinschaft is gratefully acknowledged. We thank Prof. Karl-Heinz Drexhage and Dr. Jutta Arden-Jacob, University of Siegen, for providing generous access to preparative MPLC equipment and assistance with the corresponding experiments, and Anna Bergen and Katharina Jäger, University of Siegen, for technical assistance.

- [1] J. Lhomme, J.-F. Constant, M. Demeunynck, *Biopolym. Nucl. Acid Sci.* **1999**, 52, 65–83.
- [2] O. D. Schärer, *Angew. Chem.* **2003**, 115, 3052–3082; *Angew. Chem. Int. Ed.* **2003**, 42, 2946–2974.
- [3] J.-F. Constant, M. Demeunynck in *DNA and RNA Binders: From Small Molecules to Drugs* (Eds.: M. Demeunynck, C. Bailly, W. D. Wilson), Wiley-VCH, Weinheim, **2003**, pp. 247–277.
- [4] For other strategies see: a) J. R. Bertrand, J.-J. Vasseur, A. Gouyette, B. Rayner, J. L. Imbach, C. Paoletti, C. Malvy, *J. Biol. Chem.* **1989**, 264, 14172–14178; b) C. Malvy, H. Safroui, E. Bloch, J. R. Bertrand, *Anti-Cancer Drug Des.* **1988**, 2, 361–370; c) M. Jourdan, J. Garcia, J. Lhomme, M.-P. Teulade-Fichou, J.-P. Vigneron, J.-M. Lehn, *Biochemistry* **1999**, 38, 14205–14213; d) N. Berthet, J. Michon, J. Lhomme, M.-P. Teulade-Fichou, J.-P. Vigneron, J.-M. Lehn, *Chem. Eur. J.* **1999**, 5, 3625–3630.
- [5] a) N. Berthet, J.-F. Constant, M. Demeunynck, P. Michon, J. Lhomme, *J. Med. Chem.* **1997**, 40, 3346–3352; b) P. Belmont, M. Jordan, M. Demeunynck, J.-F. Constant, J. Garcia, J. Lhomme, *J. Med. Chem.* **1999**, 42, 5153–5159.
- [6] a) J.-F. Constant, T. R. O'Connor, J. Lhomme, J. Laval, *Nucleic Acids Res.* **1988**, 16, 2691–2703; b) A. Fkyerat, M. Demeunynck, J.-F. Constant, P. Michon, J. Lhomme, *J. Am. Chem. Soc.* **1993**, 115, 9952–9959.
- [7] A. Martelli, M. Jourdan, J.-F. Constant, M. Demeunynck, P. Dumy, *Bioorg. Med. Chem. Lett.* **2006**, 16, 154–157.
- [8] H. Ihmels, K. Faulhaber, D. Vedaldi, F. Dall'Acqua, G. Viola, *Photochem. Photobiol.* **2005**, 81, 1107–1115.
- [9] C. Bohne, K. Faulhaber, B. Giese, A. Häfner, A. Hofmann, H. Ihmels, A.-K. Köhler, S. Perä, F. Schneider, M. A. L. Sheepwash, *J. Am. Chem. Soc.* **2005**, 127, 76–85.
- [10] C. K. Bradsher, J. C. Parham, *J. Heterocycl. Chem.* **1964**, 1, 30–33.
- [11] M. Bodanszky, A. Bodanszky, *The Practice of Peptide Synthesis 2nd Ed.*; Springer, New York, **1994**.
- [12] a) N. J. Leonard, K. Ito, *J. Am. Chem. Soc.* **1973**, 95, 4010–4016; b) M. Hisatome, N. Maruyama, K. Ikeda, T. Furutera, T. Ishikawa, K. Yamakawa, *Chem. Pharm. Bull.* **1996**, 44, 1801–1811.
- [13] a) A. W. McConnaughie, T. C. Jenkins, *J. Med. Chem.* **1995**, 38, 3488–3501; b) M. Aslanoglu, *Anal. Sci.* **2006**, 22, 439–443.
- [14] J. D. McGhee, P. H. von Hippel, *J. Mol. Biol.* **1974**, 86, 469–489.
- [15] H. Ihmels, K. Faulhaber, C. Sturm, G. Bringmann, K. Messer, N. Gabellini, D. Vedaldi, G. Viola, *Photochem. Photobiol.* **2001**, 74, 505–511.
- [16] In this work, the DNA concentration is expressed in base pair (bp) units in the case of polynucleotides and as concentration of oligonucleotide duplexes in the case of deoxyribooligonucleotides.
- [17] B. Nordén, T. Kurucsev, *J. Mol. Recognit.* **1994**, 7, 141–156.
- [18] a) G. Cohen, H. Eisenberg, *Biopolymers* **1969**, 8, 45–55; b) D. Suh, J. B. Chaires, *Bioorg. Med. Chem.* **1995**, 3, 723–728.
- [19] See e.g. a) C. Pena, I. Alfonso, B. Tooth, N. H. Voelcker, V. Gotor, *J. Org. Chem.* **2007**, 72, 1924–1930; b) S. Dallavalle, G. Giannini, D. Alloatti, A. Casati, E. Marastoni, L. Musso, L. Merlini, G. Morini, S. Penco, C. Pisano, S. Tinelli, M. De Cesare, G. L. Beretta, F. Zunino, *J. Med. Chem.* **2006**, 49, 5177–5186; c) S. Blanchard, I. Rodriguez, C. Tardy, B. Baldeyrou, C. Bailly, P. Colson, C. Houssier, S. Leonce, L. Kraus-Berthier, B. Pfeiffer, P. Renard, A. Pierre, P. Caubere, G. Guillaumet, *J. Med. Chem.* **2004**, 47, 978–987; d) L. Wang, H. L. Price, J. Juusola, M. Kline, O. Phanstiel II, *J. Med. Chem.* **2001**, 44, 3682–3691; e) J. Sartorius, H.-J. Schneider, *J. Chem. Soc. Perkin Trans. 2* **1997**, 2319–2327; f) J. B. Le Pecq, M. Le Bret, J. Barbet, B. Roques, *Proc. Natl. Acad. SciUSA.* **1975**, 72, 2915–2919.
- [20] W. A. Denny in *DNA and RNA Binders: From Small Molecules to Drugs* (Eds.: M. Demeunynck, C. Bailly, W. D. Wilson), Wiley-VCH, Weinheim, **2003**, pp. 482–502.
- [21] M. Hannon, A. Rodger, N. H. Mann, (Univ. Warwick); WO 2005/033119, **2005**.
- [22] a) N. J. Leonard, K. Ito, *J. Am. Chem. Soc.* **1973**, 95, 4010–4016; b) M. Hisatome, N. Maruyama, K. Ikeda, T. Furutera, T. Ishikawa, K. Yamakawa, *Chem. Pharm. Bull.* **1996**, 44, 1801–1811.
- [23] D. E. Graves in *DNA Topoisomerase Protocols: Enzymology and Drugs* (Eds.: N. Osheroff, M. A. Bjornsti), Humana Press, Totowa, NJ, **2001**, pp. 161–169.
- [24] P. C. Dedon in *Current Protocols in Nucleic Acid Chemistry* (Eds.: S. L. Beaucage, D. E. Bergstrom, G. D. Glick, R. A. Jones), John Wiley & Sons, New York, **2000**.

Received: March 8, 2007

Published Online: July 19, 2007